Analyst

RSC Publishing

PAPER

View Article Online
View Journal | View Issue

Cite this: *Analyst*, 2013, **138**, 642

A gold nanorods-based fluorescent biosensor for the detection of hepatitis B virus DNA based on fluorescence resonance energy transfer

Xiaocui Lu,[a] Xiao Dong,[a] Keying Zhang,[b] Xiaowei Han,[a] Xian Fang[a] and Yuzhong Zhang*[a]

In this study, we designed a fluorescence resonance energy transfer system containing gold nanorods (AuNRs) and fluorescein (FAM) for the detection of hepatitis B virus DNA sequences. AuNRs were synthesized according to the seed-mediated surfactant-directed approach, and the surface of the AuNRs was wrapped with a thin layer of cetyltrimethylammonium bromide (CTAB), resulting in the AuNRs being positively charged. When FAM-tagged single-stranded DNA (FAM-ssDNA) was added into the AuNRs suspension, it was adsorbed onto the surface of the positively charged AuNRs and formed a FAM-ssDNA–CTAB–AuNRs ternary complex, the resulting structure led to a fluorescence resonance energy transfer (FRET) process from FAM to AuNRs and the fluorescence intensity of FAM was consequently quenched. When complementary target DNA was added to the FAM-ssDNA–CTAB–AuNRs complex solution, a further decrease in fluorescence intensity was observed because of an increased FRET efficiency. Under optimal conditions, the decline of the fluorescence intensity of FAM (ΔF) was linear with the concentration of the complementary DNA from 0.045 to 6.0 nmol L^{-1} and the detection limit was as low as 15 pmol L^{-1} (signal/noise ratio of 3). When this fluorescent DNA sensor was used to detect the polymerase chain reaction product of hepatitis B virus gene extracted from a positive real sample, a positive response was obtained. Impressively, the biosensor exhibits good selectivity, even for single-mismatched DNA detection.

Received 10th August 2012
Accepted 3rd November 2012

DOI: 10.1039/c2an36099c

www.rsc.org/analyst

Introduction

Hepatitis B is an important health problem worldwide and the virus of hepatitis B causes acute and chronic liver diseases. An epidemiological survey has shown that at least 800 million people have been infected with hepatitis B virus (HBV), and the carrying rate of the hepatitis B surface antigen has reached 9.75% in China.[1] Therefore, it is important to develop simple, rapid and reliable methods for the diagnosis of HBV. Up to now, many methods for the detection of HBV have been reported including single strand conformation,[2] high performance liquid chromatography[3] and real-time PCR[4,5] *etc.* However, these methods still have some limitations as they are complex, time-consuming and expensive. Therefore, it is urgent to develop a simple, rapid, sensitive and selective method for the detection of HBV .

With the advent of nanotechnology, gold nanoparticles have received widespread interest in the detection of DNA owing to their unique optical properties and bioconjugation.[6,7] The pioneering work was carried out by Mirkin and his co-workers.[8] After that, a number of studies focusing on DNA detection using spherical gold nanoparticles have been reported.[9] Recently, gold nanorods (AuNRs), which are elongated gold nanoparticles, have attracted increasing attention for biotechnological applications. Compared with the spherical gold nanoparticles, AuNRs show higher absorption and stronger light scattering properties, and give two absorption peaks in the visible and near infrared regions, which correspond to the transverse and longitudinal surface plasmon bands, respectively.[10,11] The longitudinal surface plasmon band is extremely sensitive to changes in the dielectric properties of the surroundings including solvents, adsorbates, and the inter-particle distance of the AuNRs. In addition, the surface of AuNRs can easily be modified. Therefore, AuNRs have been explored for potential applications in biosensor[12–14] gene delivery[15,16] and photothermal therapy.[17–19] For example, Darbha *et al.* utilized the second-order nonlinear optical properties of AuNRs to screen the HIV-1 viral DNA sequence with a sensitivity of about 100 pmol L^{-1},[20] Parab *et al.* reported

[a]*College of Chemistry and Materials Science, Anhui Key Laboratory of Chemo-Biosensing, Anhui Normal University, Wuhu 241000, People's Republic of China. E-mail: zhyz65@mail.ahnu.edu.cn; Fax: +86 553 3869303; Tel: +86 553 3869303*

[b]*Department of Chemistry-Biology, Anhui Key Laboratory of Spin Electron and Nanomaterials (Cultivating Base), Suzhou University, Suzhou, Anhui 234000, People's Republic of China*

an AuNRs-based optical DNA biosensor for the diagnosis of pathogens.[21]

Fluorescence resonance energy transfer (FRET) often occurs when there is appreciable overlap between the emission spectrum of the donor and the absorption spectrum of the acceptor. In this process, the emission energy of the donor is absorbed by the acceptor. FRET has been employed as a powerful tool for the study of biological macromolecules, and has shown prominent sensitivity in quantitative analysis.[22] As is well known, the emission spectrum of fluorescein (FAM) and the absorption spectrum of the AuNRs represent appreciable overlap, FRET can occur from FAM to AuNRs (herein, FAM is the donor and AuNRs is the acceptor). In this study, we reported an AuNRs-based fluorescent biosensor for the detection of HBV sequences, and FAM-ssDNA was selected as the probe DNA. When probe DNA was added into AuNRs suspension, the fluorescence intensity of FAM decreased due to the FRET which occured from FAM to AuNRs, when the complementary DNA was added into the system, the fluorescence intensity of FAM was further decreased which was ascribed to the strengthened electrostatic interaction and increased FRET efficiency. Under optimal conditions, the decline of the fluorescence intensity of FAM was linearly related to the concentration of the complementary DNA in the range from 0.045 to 6.0 nmol L^{-1}, and the detection of polymerase chain reaction (PCR) product of HBV gene also gave a satisfactory result. The protocol of the biosensor is shown in Scheme 1.

Experimental

Chemicals and reagents

Chloroauric acid ($HAuCl_4 \cdot 4H_2O$) was obtained from Shanghai Chemical Reagent Co., Ltd. Cetyltrimethylammonium bromide (CTAB), silver nitrate ($AgNO_3$), sodium chloride (NaCl), ascorbic acid (AA) and sodium borohydride ($NaBH_4$) were purchased from Sinopharm Chemical Reagent Co., Ltd (Shanghai, China). The sequences of oligonucleotides were purchased from Shanghai Sangon Inc. (Shanghai, China). All sequences are listed as follows:

Probe sequences (FAM-ssDNA): 5′-AAT GTG CTC CCC CAA CTC CTC-6-FAM-3′

Complementary sequences (cDNA): 5′-GAG GAG TTG GGG GAG CAC ATT-3′

Non-complementary sequences: 5′-AAA AGG TGT AAG CGT TTG CCG-3′

Single-mismatched sequences: 5′-GAG GAG TTG NGG GAG CAC ATT-3′

("N" stands for A, T, or C)

The oligonucleotide primers for HBV are listed as follows:

HBV primer 1: 5′-TAG CAG GCT GTA GGC ATA AAT TGG T-3′

HBV primer 2: 5′-GGC GAG GGA GTT CTT CTT CTA GGG G-3′

All oligonucleotide stock solutions were prepared with 0.01 mol L^{-1} phosphate buffer saline (PBS, pH 7.40) and were stored in a refrigerator. Hybridization buffer solution (0.01 mol L^{-1} PBS + 0.20 mol L^{-1} NaCl, pH 7.40) was used. All chemicals were of analytical grade and were used without further purification. All solutions were prepared with twice-quartz-distilled water.

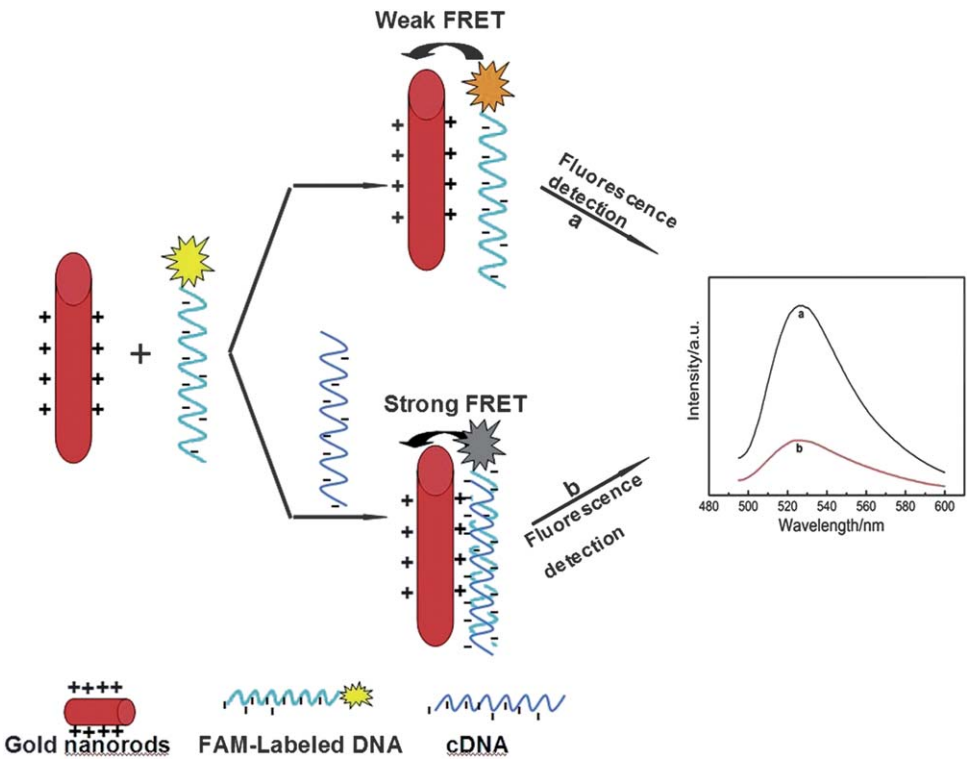

Scheme 1 Schematic representation of the strategy for DNA hybridization detection.

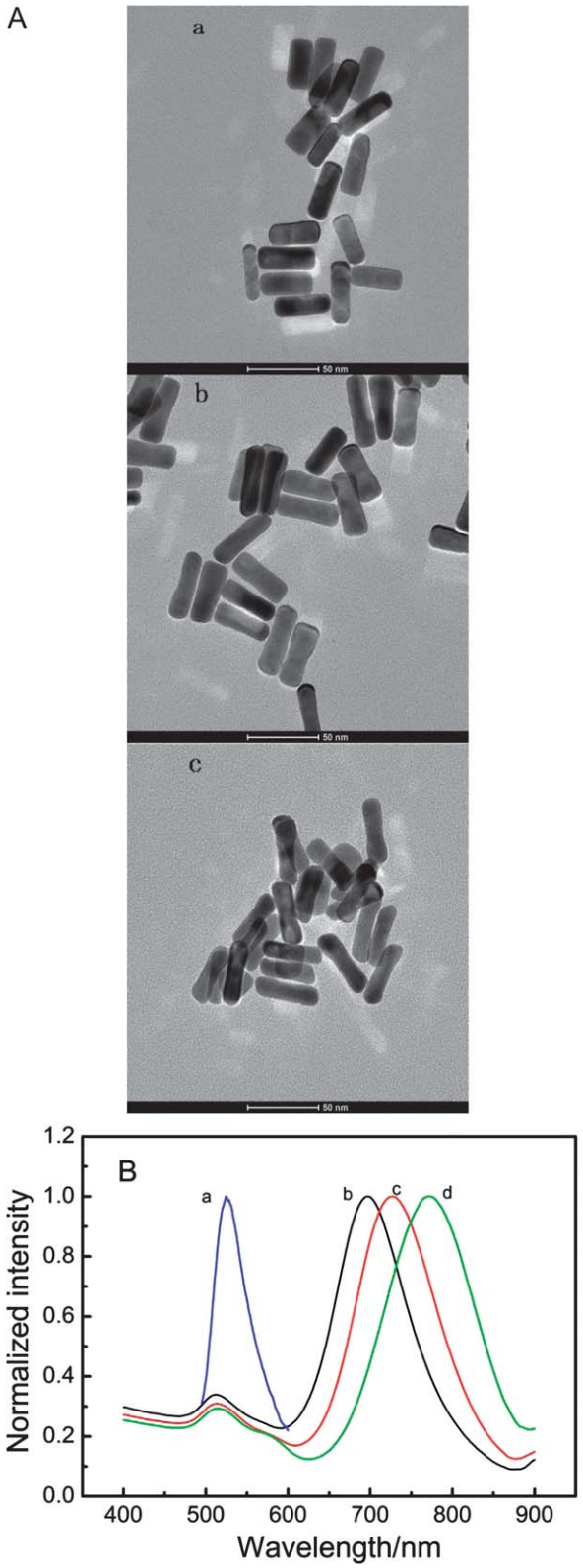

Fig. 1 (A) TEM images of the different aspect ratios of AuNRs (the aspect ratios of AuNRs were 2.7, 3.2 and 3.6 from a to c). (B) Normalized SPR absorption spectrum of AuNRs with three different aspect ratios (b-2.7, c-3.2 and d-3.6) and emission spectrum of FAM-ssDNA (a).

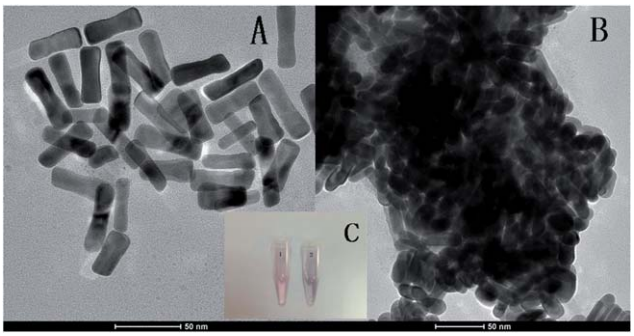

Fig. 2 TEM images of FAM-ssDNA–CTAB–AuNRs conjugates before (A) and after hybridization with cDNA (B) at 37 °C. The color of FAM-ssDNA–CTAB–AuNRs conjugates changes from red to light purple (C). Red denotes the color of ternary complexes and light purple denotes the color after hybridization with target DNA. Condition: $C_{FAM\text{-}ssDNA} = 6.0$ nmol L^{-1}, $C_{cDNA} = 6.0$ nmol L^{-1}.

Instruments

All fluorescence measurements were performed on an F-4500 fluorescence spectrophotometer (Hitachi, Japan). The UV-vis-NIR absorption spectra were obtained on a U-3010 UV-vis-NIR spectrometer (Hitachi, Japan). A transmission electron microscope (TEM) (Hitachi-800) was used to obtain images of the AuNRs.

Preparation of gold nanorods

AuNRs were synthesized in aqueous solution with reference to the seed-mediated method as reported by Murphy and others.[23–25] Briefly, the seed solution was prepared by mixing CTAB (2.5 mL, 0.20 mol L^{-1}) and $HAuCl_4$ (2.5 mL, 5.0×10^{-4} mol L^{-1}) with ice-cold $NaBH_4$ (0.30 mL, 0.01 mol L^{-1}), After 2 h, this seed solution was used for the synthesis of AuNRs.

In one flask, CTAB (10 mL, 0.20 mol L^{-1}) was mixed with $AgNO_3$ solution (0.10, 0.20, 0.40 mL and 4.0×10^{-3} mol L^{-1}) and $HAuCl_4$ (10.0 mL and 1.0×10^{-3} mol L^{-1}). After gentle mixing of the solution, 140 μL AA (0.0788 mol L^{-1}) was added to this system. Then, 24 μL of the seed solution was added to the growth solution to initiate the growth of AuNRs, and the temperature of the solution was kept constant at 30 °C for 24 h. Afterwards, excess CTAB was removed from the solution by centrifugation at a rate of 8000 rpm for 10 min and the AuNRs were re-dispersed in distilled water.

DNA hybridization and fluorescence detection

The DNA hybridization experiment was carried out at 37 °C. Typically, 6 μL of probe DNA (1.0×10^{-6} mol L^{-1}) was added to 904 μL of PBS containing 0.2 mol L^{-1} NaCl, then, 30 μL of AuNRs were added to the mixed solution. After the mixed solution was vigorously stirred for 5 min, a suitable target DNA was added to the mixture above and reacted for 50 min at 37 °C (the solution volume was 1 mL in total). The fluorescence detection was performed at excitation and emission wavelengths of 480 nm and 524 nm, respectively. And the concentration of complementary DNA was quantified by the decline of

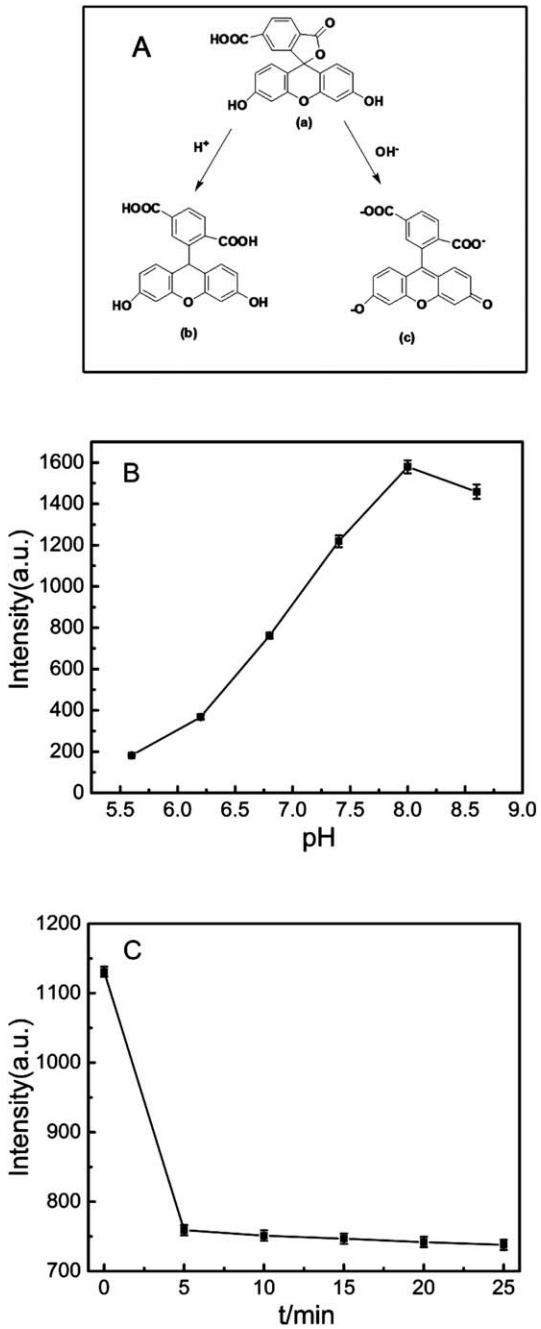

Fig. 3 (A) Mechanism of pH influence on the FAM structure. (B) Effect of pH on fluorescence intensity of FAM. (C) Effect of the reaction time between FAM-ssDNA and AuNRs on fluorescence intensity of FAM. Conditions: $C_{\text{FAM-ssDNA}} = 6.0$ nmol L^{-1}, $V_{\text{AuNRs}} = 30$ μL.

FAM fluorescence intensity before and after DNA hybridization ($\Delta F = F_{\text{ssDNA}} - F_{\text{dsDNA}}$).

PCR amplification of DNA from blood samples

DNA was extracted from venous blood by using a TIANamp Genomic DNA kit purchased from Tiangen Biotech Co., Ltd (Beijing China). The PCR amplification was performed in a Bio-Rad PCR cycler (Perkin-Elmer Cetus) using oligonucleotide primer.

During the PCR process, after a first step of denaturation at 95 °C for 5 min, each of the 35 cycles of amplification consisted of 1 min of primer annealing at 60 °C, 2 min of extension at 70 °C. The amplification products of HBV were 595 bp (base pair) fragments. The PCR products were diluted with buffered saline and thermally denatured by using a boiling water bath (5 min at 95 °C). The amplicon strands re-annealing was then retarded by cooling the sample in an ice-water bath for 5 min and followed by fluorescent sensor detection using the same procedure as for the synthetic oligonucleotides. 2.5 μL each of the PCR products were analyzed by electrophoresis separation on a 2% agarose gel containing ethidium bromide in TAE buffer.

Results and discussion

Characterization of gold nanorods

TEM was used to observe the morphology of the AuNRs, and the TEM images of different aspect ratios of the AuNRs (2.7 : 1, 3.2 : 1 and 3.6 : 1) are shown in Fig. 1A. It can be seen that the AuNRs are highly dispersed and there is no aggregation. The UV-vis spectrum of the as-prepared AuNRs exhibit two distinct plasmon absorption bands centered at 518 and 700 nm (curve b in Fig. 1B), which are assigned to the transverse and longitudinal plasmon resonance absorption (PRA) of the AuNRs, respectively. With the increase of aspect ratio, the longitudinal absorption peak was red-shifted from 700 to 770 nm.

Sensing mechanism

The AuNRs include a metallic core surrounded by a CTAB surfactant. The head group of the surfactant is a quaternary amine, which has a positive charge on the nitrogen and a solvated bromide as the counterion, which can be in close proximity to the positive charge on the nitrogen or far from the surface of the nanoparticle. Therefore, AuNRs have a large number of positive charges on their surface. When FAM-ssDNA was added to the AuNRs suspension, probe DNA was adsorbed onto the surface of the positively charge AuNRs, and ternary FAM-ssDNA–CTAB–AuNRs complexes were formed. FRET occurs when there is appreciable overlap between the emission spectrum of the donor and the absorption spectrum of the acceptor. AuNRs can act as electron acceptors to quench fluorophores in the photoinduced electron transfer process because the AuNRs have an absorption peak which overlaps with the emission peak of FAM (seen in Fig. 1B).

As is well known, the FRET process is extremely distance dependent, the relationship of FRET efficiency (E_{FRET}) with the distance between acceptor and donor is expressed as[26]

$$E_{\text{FRET}} = [1 + (R_{\text{DA}}/R_0)^6]^{-1} \quad (1)$$

where R_{DA} represents the distance between the donor and acceptor, R_0 is the distance at which the efficiency of transfer reaches 50%. E_{FRET} decreases rapidly with an increase of R_{DA}. Generally, FRET occurs easily when the distance between the donor and acceptor is 7 to 10 nm. The bilayer of CTAB on the surface of AuNRs is about 4 nm thick,[27] allowing the FRET

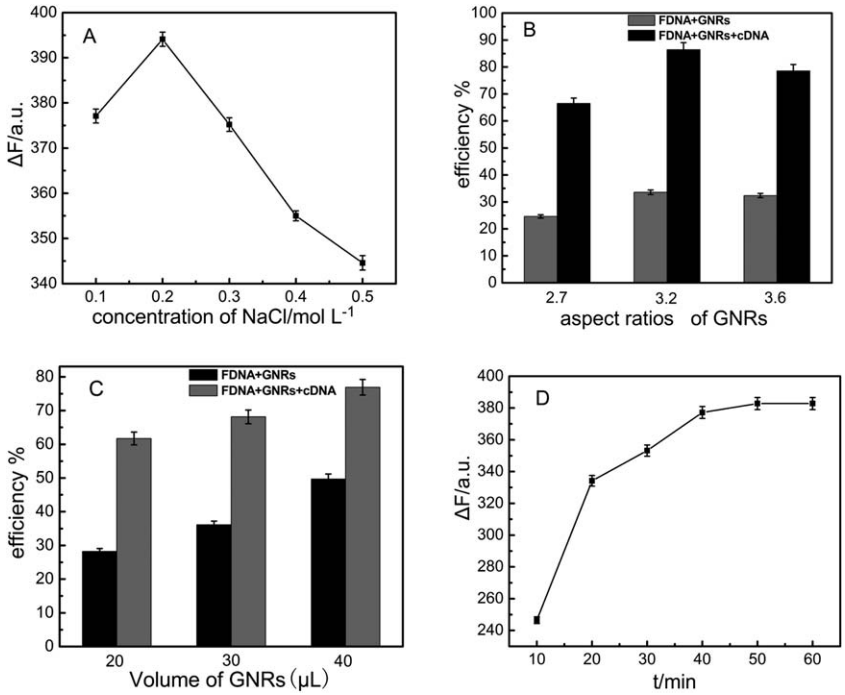

Fig. 4 (A) Effect of the ionic strength on the DNA hybridization (NaCl concentration: 0.10, 0.20, 0.30, 0.40 and 0.50 mol L^{-1}). (B) Effect of the aspect ratio of AuNRs on FRET efficiency (the aspect ratios of AuNRs were 2.7, 3.2, and 3.6, respectively). (C) Effect of amount of AuNRs on FRET efficiency. (D) The relationship between the fluorescence intensity and hybridization time. Condition: $C_{FAM\text{-}ssDNA} = 6.0$ nmol L^{-1}, $C_{cDNA} = 3.5$ nmol L^{-1} (A, C and D), $C_{cDNA} = 6.0$ nmol L^{-1} (B). The efficiency is obtained according to the expression $E = F_0 - F/F_0$, where F_0 is the fluorescence intensity of FAM-ssDNA, F is the fluorescence intensity of FAM when AuNRs (grey), or target DNA sequences (black) have been added.

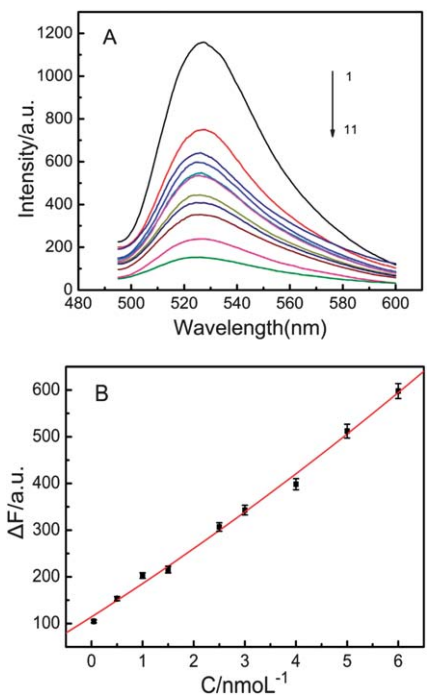

Fig. 5 (A) Fluorescence spectra of FAM-ssDNA (1), FAM-ssDNA–CTAB–AuNRs conjugates (2) and hybridized with various concentrations of cDNA (3–11). (B) The plot of analytical signal *versus* the concentration of cDNA in the range of 0.045 to 6.0 nmol L^{-1}.

process to take place between the FAM-ssDNA and AuNRs with moderate transfer efficiency. Fig. 1B shows the normalized surface plasmon resonance (SPR) absorption spectrum of AuNRs with three different aspect ratios and the emission spectra of the FAM-ssDNA. It is clearly observed that there is overlap between the emission spectra of FAM-ssDNA and plasmon absorption bands of AuNRs, which make it is possible for FRET to occur from FAM to AuNRs. When the cDNA was added into the system, the fluorescence intensity of FAM decreased rapidly because of the formation of the FAM-ssDNA/cDNA duplex which has a more negative charge density in contrast to FAM-ssDNA and gives rise to stronger electrostatic interactions between the FAM-ssDNA/cDNA duplex and AuNRs. Consequently, the distance between the FAM units and AuNRs is reduced, which gives rise to more efficient FRET from the FAM to the AuNRs.

TEM was used to demonstrate the sensing mechanism. Fig. 2 shows the TEM images of FAM-ssDNA–CTAB–AuNRs conjugates before (A) and after hybridization with cDNA (B). It is clearly observed that the FAM-ssDNA–CTAB–AuNRs conjugates are well dispersed, and the electrostatic interaction is not strong enough to change the suspension state of AuNRs. In the presence of cDNA, AuNRs obviously aggregated (Fig. 2B) this is ascribed to dsDNA having a higher density of negative charge, and the electrostatic interaction between dsDNA and AuNRs was strengthened. Therefore, the distance between dsDNA and AuNRs became shorter, leading to an increase of FRET efficiency. When probe DNA hybridized with 6 nmol L^{-1} of cDNA,

Table 1 Comparison of various AuNRs-based DNA biosensors

The analytical methods of DNA detection	Linear range/nmol L^{-1}	LOD[a]/nmol L^{-1}	Real sample	Ref.
Gold-nanorod-based sensing of sequence specific HIV-1 virus DNA by using hyper-Rayleigh scattering spectroscopy	0.1–50	0.10	—	21
Monitoring human telomere DNA hybridization and G-quadruplex formation using gold nanorods	13.4–67	4.47	—	27
One-step lable-free optical genosensing system for sequence-specific DNA related to the human immunodeficiency virus based on the measurements of light scattering signals of gold nanorods	0.17–11.67	0.080	HIV-1 LTR real sample	30
A gold nanorod-based optical DNA biosensor for the diagnosis of pathogens	0.25–75	0.083	Human urine sample	31
A gold nanorods–based fluorescent biosensor for the detection of hepatitis B virus DNA based on fluorescence resonance energy transfer	0.045–6	0.015	Human urine sample	This work

[a] The mean of three determinations.

the color of the mixture changed from red to light purple and this was clearly observed (Fig. 2C). The reason is that the transverse PRA band shows a weak hyperchromic effect and gets slightly red-shifted, while the longitudinal PRA band displays obvious hypochromic and hypsochromic effects with the addition of target DNA to the mixture of probe DNA and AuNRs suspension.

Optimization of experimental conditions

In this work, the effect of assay conditions (such as pH, ionic strength, reaction time between FAM-ssDNA and AuNRs *et al.*) on the experimental results was investigated. FAM is a pH-sensitive fluorophore and its quantum yield is close to zero when the pH is lower than 4.[28] The mechanism of pH influence on the FAM is shown in Fig. 3A. When the pH is lower than 7, the molecular structure of FAM converts from (a) to (b) leading to the destruction of the conjugate system of FAM, and a dramatic decrease of fluorescence intensity of FAM. It is obviously observed that the fluorescence intensity of FAM increases with an increase of the pH of solution; when the pH is higher than 7, the molecular structure of FAM converts from (a) to (c), and the conjugate system of FAM increases. The effect of solution pH on the analytical signal is shown in Fig. 3B, in this study we selected buffers of pH 7.4 as this is close to the physiological pH value.

The effect of reaction time of FAM-ssDNA and AuNRs on analytical signal is shown in Fig. 3C. The fluorescence intensity of FAM decreased clearly within 5 min, and decreased slowly from 5 to 25 min. Hence, 5 min reaction time was chosen in this study.

The ionic strength of the solution is an important factor for the hybridization reaction. Studies previously showed that the stability of CTAB–AuNRs composite was better even in a high ionic strength solution (such as 0.50 mol L^{-1} NaCl),[29] the effect of ionic strength on analytical signal in this study was also investigated and is shown in Fig. 4A. The value of the fluorescence intensity (ΔF) increased significantly with increasing concentration of NaCl (0.1 to 0.2 mol L^{-1}), and decreased over 0.2 mol L^{-1}. So, 0.20 mol L^{-1} NaCl solution was used for this study.

The effect of the aspect ratio of the AuNRs on analytical signal was investigated and the results are shown in Fig. 4B. It can be observed that the aspect ratio of the AuNRs obviously affected FRET efficiency and the FRET efficiency the highest when the aspect ratio of the AuNRs was 3.2. The AuNRs (the aspect ratio of AuNRs is 3.2) exhibit two obvious surface plasmon bands centered at 519 nm and 734 nm, which are assigned to the transverse and longitudinal surface plasmon bands of the AuNRs, respectively. FAM possesses an emission maximum at 524 nm. The emission peak of FAM overlapped well with the absorbance peak of the AuNRs, resulting in FRET process taking place. The effect of the amount of AuNRs was investigated and is shown in Fig. 4C. From Fig. 4C, it can be observed that a volume of 20 μL of AuNRs has a higher FRET efficiency (33.49%) than that of 30 μL of AuNRs (32.01%) (the FRET efficiency data

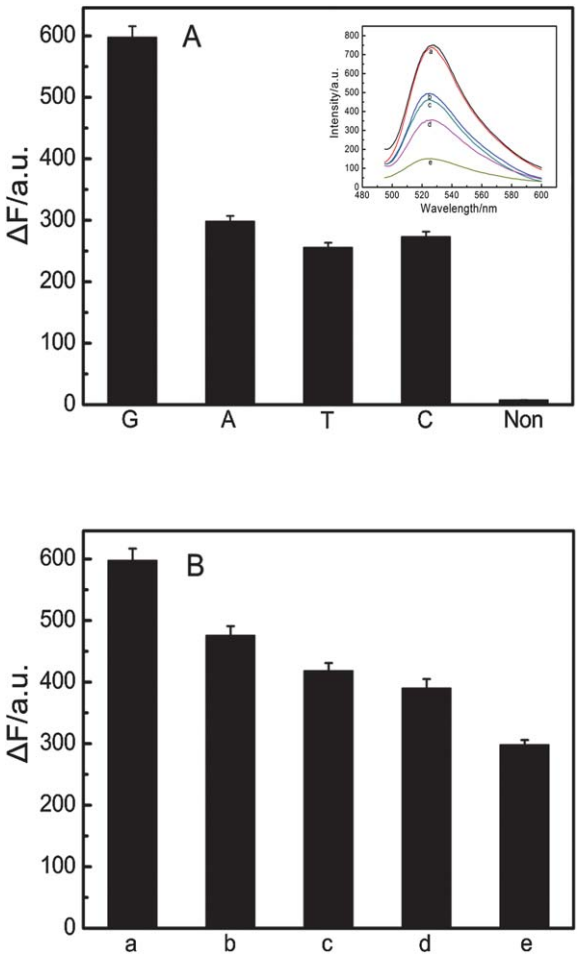

Fig. 6 (A) Histograms of the decrease of fluorescence intensity of probe DNA hybridization with different DNA sequences: non-complementary sequences (non); single-base mismatched sequences (A, T and C); complete complementary sequences (G). Inset: the fluorescence curves of FAM-ssDNA hybridized with different DNA sequences. Black curve, probe DNA; a, non-complementary sequences; b, c, d, single-base mismatched sequences and e, complete complementary sequences. Conditions: $C_{FAM\text{-}ssDNA}$ = 6.0 nmol L^{-1}, the concentration of the target DNA were 6.0 nmol L^{-1}. (B) Histograms of the analytical signal of different ratios of single-base mismatched ("N" stands A) to complementary DNA: 1 : 1 (b), 10 : 1 (c), 100 : 1 (d); control experiments: 6.0 nmol L^{-1} complete complementary sequences (a) and 6.0 nmol L^{-1} single-base mismatched sequences (e).

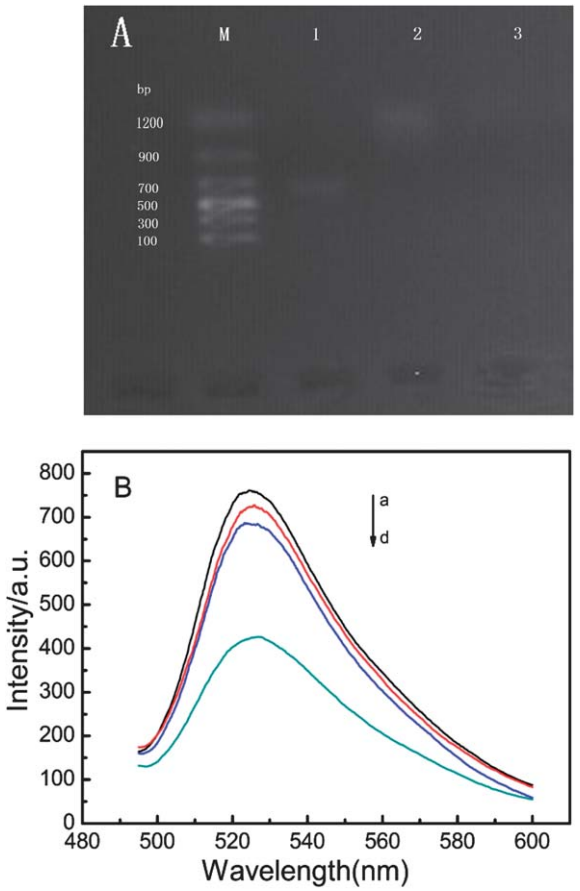

Fig. 7 (A) Electrophoresis image of PCR products. The lanes from left to right: (M) DNA marker, (1) positive real sample, (2) negative real sample, (3) PCR blank solution. (B) Fluorescent curves of FAM-ssDNA–CTAB–AuNRs conjugates (a), and after hybridization with PCR blank solution (b), negative real sample PCR product (c), positive real sample PCR product (d).

obtained subtract the value of AuNRs decreased the fluorescence intensity of FAM). In addition, we investigated the effect of the amount of AuNRs on analytical performance (linear range), we found that the linear range was wider when 30 μL of AuNRs was used. From the view of linear range, we selected 30 μL of AuNRs for this study. Hybridization time was investigated in this study and the results are shown in Fig. 4D. From the results presented in Fig. 4D, 50 min was selected as the hybridization time for this study.

Analytical performance

Under the optimal conditions, the analytical performance of the fluorescent DNA biosensor was investigated using the probe DNA to hybridize with different concentrations of cDNA sequences. Fig. 5A shows the fluorescence spectrums of FAM at different concentrations of cDNA sequences. The decline of fluorescence intensity of FAM increased with an increasing of the concentrations of cDNA and was linear realtive to the concentration of cDNA from 0.045 to 6.0 nmol L^{-1} with a correlation coefficient of 0.9961 (as seen in Fig. 5B). The linear regression equation was $\Delta F = 101.20105 + 81.15942\ C_{cDNA}$ (unit of C is nmol L^{-1}). A detection limit of 15 pmol L^{-1} was estimated at a signal/noise ratio of 3. We have also consulted some literature on the use of AuNRs-based optical biosensors to detect target DNA and the data is shown in Table 1. From the view of sensitivity, the biosensor possessed higher sensitivity in contrast to work previously reported.

Selectivity of the biosensor

The selectivity of the biosensor was evaluated using probe DNA to hybridize with non-complementary sequences (non), single-base mismatched sequences (A, T and C) and complete complementary sequences (G), and the fluorescence spectrum of FAM were recorded and are presented in Fig. 6A. The

histograms of decline of fluorescence intensity *vs.* different sequences DNA are shown in Fig. 6A. For the non-complementary DNA sequences, the value obtained was the lowest because the non-complementary DNA could not be hybridized with the probe DNA; for all single-base mismatched sequences, the values obtained were lower than 50% of the complementary sequences. These results indicated that the biosensor could distinguish single-base mismatched DNA sequences from non-complementary and complementary sequences.

To further assess the specificity of our method, the single-base mismatched sequences and complementary sequences were mixed together at different mole ratios of 1 : 1, 10 : 1 and 100 : 1 with a total concentration of 6 nmol L^{-1} (seen in Fig. 6B). As shown in Fig. 6B, the signal decreased sharply when the mole ratio increased from 1 : 1 to 10 : 1 and decreased slowly from 10 : 1 to 100 : 1. Obvious changes of fluorescence intensity could be observed even when the single-base mismatched sequences to complementary sequences 100 : 1 (the complementary DNA is about 0.0594 nmol L^{-1}). This result indicated that the complementary sequences could be detected in the presence of 100-fold excess single-base mismatched sequences.

Detection of PCR product of HBV sequences

The human blood samples were kindly donated by Yiji Shan Hospital of Wuhu. The HBV gene was extracted from the samples and the PCR process was carried out according to the process described previously. The denatured HBV gene fragment from PCR amplification was used as the target DNA for the analysis. The electrophoresis control matrix for HBV is given in Fig. 7A. The positive real sample (lane 1) gave a final PCR product with the gene fragment length of 595 bp, while the negative real sample (lane 2) and PCR blank solution (lane 3) did not show the light brand.

Fig. 7B shows the fluorescence curves of FAM when the probe hybridized with real PCR samples. An obvious decrease was obtained in fluorescence intensity of FAM for the positive sample (d), the negative sample (c) did not contain complementary sequences to the probe, and the hybridization could not occur, so fluorescence intensity of FAM showed only a slightly decrease of FAM. The blank solution of PCR (b) was also used as a target solution to examine the effect on the FAM signal, the signal obtained was nearly as high as the probe signal (a). The significant changes of the fluorescence intensity of FAM confirmed that this fluorescent DNA biosensor could effectively detect the PCR product of HBV gene, and has potential application for use in the detection of the HBV gene. The results obtained for this fluorescence biosensor were consistent with those obtained using gel electrophoresis.

Conclusions

In this work, we designed an AuNRs-based fluorescent biosensor for the detection of hepatitis B virus DNA. TEM was used to obtain images of the AuNRs and the experimental conditions were optimized. The obtained biosensor could detect the complementary sequences from 0.045 to 6.0 nmol L^{-1} with a detection limit of 15 pmol L^{-1}, in addition, the detection of the PCR product of the HBV gene also gave a satisfactory result. At the times, the studies provide a platform for AuNRs application in biological system.

Acknowledgements

This work was financially supported by the National Natural Science Foundation of China (no. 20675002) and the Natural Science Foundation of Anhui Province (no. 1208085QB33). The authors are thankful for the kind help from Prof. Liuwang Nie with sample treatment and preparation of PCR products, and Prof. Yunsheng Xia who carefully read this manuscript.

References

1 N. L. Zou, Y. C. Zang, H. J. Mao, G. Q. Zhao, Q. H. Jin, J. L. Zhao and Y. S. Xu, *Chin. J. Anal. Chem.*, 2012, **40**, 569–573.
2 T. Sasaki, T. Tahira, A. Suzuki, K. Higasa, Y. Kukita, S. Basa and K. Hayashi, *Am. J. Hum. Genet.*, 2001, **68**, 214–218.
3 J. Wolford, D. Blunt, C. Ballecer and M. Prochazka, *Hum. Genet.*, 2000, **107**, 483–487.
4 H. F. Geng, B. Hua, H. Wang, Y. H. Cao, Y. Sun and A. R. Yu, *J. Virol. Methods*, 2006, **132**, 25–31.
5 F. Wightman, T. Walters, A. Ayres, S. Bowden, A. Bartholomeusz, D. Lau, S. Locarnini and S. R. Lewin, *J. Clin. Microbiol.*, 2004, **42**, 3809–3812.
6 D. Pissuwan, T. Niidome and M. B. Cortie, *J. Controlled Release*, 2011, **149**, 65–71.
7 B. P. Timko, T. Dvir and D. S. Kohane, *Adv. Mater.*, 2010, **22**, 4925–4943.
8 R. Elghanian, J. J. Storhoff, R. C. Mucic, R. L. Letsinger and C. A. Mirkin, *Science*, 1997, **277**, 1078–1081.
9 C. S. Thaxton, D. G. Georganopoulou and C. A. Mirkin, *Clin. Chim. Acta*, 2006, **363**, 120–126.
10 A. Brioude, X. C. Jiang and M. P. Pileni, *J. Phys. Chem. B*, 2005, **109**, 13138–13142.
11 C. J. Murphy, T. K. Sau, A. M. Gole, C. J. Orendorff, J. X. Gao, L. F. Gou, S. E. Hunyadi and T. Li, *J. Phys. Chem. B*, 2005, **109**, 13857–13870.
12 X. Liu, Q. Dai, L. Austin, J. Coutts, G. Knowles, J. H. Zou, H. Chen and Q. Huo, *J. Am. Chem. Soc.*, 2008, **130**, 2780–2782.
13 C. D. Chen, S. F. Cheng, L. K. Chau and C. R. C. Wang, *Biosens. Bioelectron.*, 2007, **22**, 926–932.
14 C. X. Yu and J. Irudayaraj, *Anal. Chem.*, 2007, **79**, 572–579.
15 A. K. Salem, P. C. Searson and K. W. Leong, *Nat. Mater.*, 2003, **2**, 668–671.
16 C. C. Chen, Y. P. Lin, C. W. Wang, H. C. Tzeng, C. H. Wu, Y. C. Chen, C. P. Chen, L. C. Chen and Y. C. Wu, *J. Am. Chem. Soc.*, 2006, **128**, 3709–3715.
17 C. M. Reisinger, X. W. Wang and B. List, *Angew. Chem., Int. Ed.*, 2008, **47**, 8112–8115.
18 X. H. Huang, P. K. Jain, I. H. El-Sayed and M. A. El-Sayed, *Nanomedicine*, 2007, **2**, 681–693.

19 T. B. Huff, L. Tong, Y. Zhao, M. N. Hansen, J. X. Cheng and A. Wei, *Nanomedicine*, 2007, **2**, 125–132.
20 G. K. Darbha, U. S. Rai, A. K. Singh and P. C. Ray, *Chem.–Eur. J.*, 2008, **14**, 3896–3903.
21 H. J. Paraba, C. Junga, J. H. Leeb and H. G. Parka, *Biosens. Bioelectron.*, 2010, **26**, 667–673.
22 Y. S. Xia, L. Song and C. Q. Zhu, *Anal. Chem.*, 2011, **83**, 1401–1407.
23 T. K. Sau and T. K. Murphy, *Langmuir*, 2004, **20**, 6414–6420.
24 X. C. Jiang, A. Brioude and M. P. Pileni, *Colloids Surf., A*, 2006, **277**, 201–206.
25 B. Nikoobakht and M. A. El-Sayed, *Chem. Mater.*, 2003, **15**, 1957–1962.
26 S. Ranjit, K. Gurunathan and M. Levitus, *J. Phys. Chem. B*, 2009, **113**, 7861–7866.
27 X. C. Gou, J. Liu and H. L. Zhang, *Anal. Chim. Acta*, 2010, **668**, 208–214.
28 M. Wu, R. Kempaiah, P. J. J. Huang, V. Maheshwari and J. W. Liu, *Langmuir*, 2011, **27**, 2731–2738.
29 H. X. Li and L. Rothberg, *Proc. Natl. Acad. Sci. U. S. A.*, 2004, **101**, 14036–14039.
30 W. He, C. Z. Huang, Y. F. Li, J. P. Xie, R. G. Yang, P. F. Zhou and J. Wang, *Anal. Chem.*, 2008, **80**, 8424–8430.
31 H. J. Parab, C. Jung, J. H. Lee and H. G. Park, *Biosens. Bioelectron.*, 2010, **26**, 667–673.

